Full Text View

Volume 30, Issue 11 (November 2000)

Journal of Physical Oceanography
Article: pp. 2853–2865 | Abstract | PDF (412K)

Deep Pacific Circulation Controlled by Vertical Diffusivity at the Lower Thermocline Depths

Hiroyuki Tsujino, Hiroyasu Hasumi, and Nobuo Suginohara

Center for Climate System Research, University of Tokyo, Tokyo, Japan

(Manuscript received April 5, 1999, in final form January 3, 2000)

DOI: 10.1175/1520-0485(2001)031<2853:DPCCBV>2.0.CO;2

ABSTRACT

Deep Pacific circulation is investigated by using a World Ocean model with depth-dependent vertical diffusivity. Vertical diffusivity estimated from observations, 0.1×10^{-4} m^2 s^{-1} for the upper layer and 3.0×10^{-4} m^2 s^{-1} for the bottom layer, is adopted. Comparison is made between cases with different vertical diffusivity at middepths. With larger vertical diffusivity at middepths, the deep Pacific circulation becomes stronger. This is due to enhanced heat exchange between the thermocline water and the deep water through more intense diffusion at middepths. The water below the thermocline is warmed and that at the thermocline is cooled for the whole basin. The warmed deep water leads to larger heat loss through the sea surface, causing the enhanced deep-water formation in the deep-water formation region. On the other hand, the cooled thermocline water leads to larger heat gain through the sea surface where the thermocline water outcrops, counterbalancing the larger heat loss in the deep-water formation region. The deep water brought up to the middepths does not further upwell to the sea surface due to the small upper-layer vertical diffusivity, but it flows back to the deep-water formation region, slowly upwelling within the middepths. In this way, the enhanced meridional overturning forms in the deep Pacific. The layered deep Pacific meridional circulation is realistically reproduced when vertical diffusivity is larger at middepths. This circulation yields tracer distributions that compare well with observations. Such a strong deep Pacific circulation does not occur when vertical diffusivity is taken larger at middepths but is held constant below the middepths. For realistic reproduction of the deep Pacific circulation, vertical diffusivity needs to keep increasing with depth beginning at the lower thermocline depths.

1. Introduction

Thermohaline circulation is driven by the distribution of the heat and the freshwater flux through the sea surface. It takes the form that a high density water formed by convection in the very narrow region upwells in the rest of the ocean to counterbalance downward heat conduction from the sea surface (e.g., Suginohara and Aoki 1991). Since no extensive dense water formation occurs that leads to strong thermohaline circulation in the northern North Pacific, the deep and the bottom layer of the Pacific is filled with Circumpolar Deep Water (CDW) from the Southern Ocean, which is a mixture of North Atlantic Deep Water (NADW) formed in the northern North Atlantic and Antarctic Bottom Water (AABW) formed in the marginal seas of the Southern Ocean such as the Weddell Sea. The CDW flows into the Pacific at the bottom, slowly upwells, and finally flows back to the Southern Ocean at middepths (Wunsch et al. 1983). For the northward transport of CDW in the Pacific, Wunsch et al. (1983) estimated 12 Sv (Sv $\equiv 10^6$ m^3 s^{-1}) in the South Pacific from *Scorpio* data by using an inverse method. Roemmich et al. (1991) and Wijffels et al. (1996) pointed out that about 10 Sv of CDW enters the North Pacific. Recently, Roemmich et al. (1996) and Rudnick (1997) obtained a northward abyssal transport of about 10 Sv through the Samoan Passage, supporting the above estimates. There is general agreement that 10~20 Sv of CDW enters the South Pacific and about 10 Sv of it returns to the Southern Ocean at middepths. There is also agreement that about 10 Sv of CDW crosses the equator and returns to the Southern Ocean as silicate-rich deep water (Schmitz 1995). This meridional circulation pattern in the deep Pacific is often referred to as the layered deep Pacific meridional circulation (e.g., Obata et al. 1996).

Numerical models have not reproduced the deep Pacific circulation with such a large amount of transport when vertically uniform vertical diffusivity less than 0.5×10^{-4} m^2 s^{-1} is used (e.g., Nakata and Suginohara 1998; Hasumi and Suginohara 1999a). In GFDL models where depth-dependent vertical diffusivity, 0.3×10^{-4} m^2 s^{-1} in the upper layer and 1.3×10^{-4} m^2 s^{-1} in the bottom layer, is used (Bryan and Lewis 1979), the inflow of CDW into the Pacific is not large, at most 9 Sv for the Indo–Pacific sector (e.g., England 1993). Although there are some simulations where a realistic amount of transport is obtained, these simulations are artificial. Toggweiler and Samuels (1993) obtained an 8 Sv inflow of CDW into the North Pacific, but they artificially increased the formation rate of bottom water by adopting high reference salinity (35.0 psu) in the Weddell Sea and the Ross Sea for the surface restoring boundary condition. Maier-Reimer et al. (1993) obtained a 10 Sv inflow of CDW into the North Pacific in the Hamburg model, but most of it upwells to the sea surface near the equator because of large numerical diffusion arising from the upcurrent differencing scheme used in the tracer equations. The layered deep Pacific meridional circulation is formed in most of the models, although it is not so conspicuous.

Care needs to be used so that a transport estimated from observation is not the one obtained by zonal integration along constant depth surfaces but the one obtained by zonal integration along constant density surfaces. In the geostrophic transport calculation using zonal section data, a meridional transport of water mass for a certain density range is usually obtained. Thus the zonal gradient of isopycnal surface is naturally taken into account. On the other hand, the meridional transport streamfunction usually used in presenting results of numerical models is obtained by zonal integration of meridional velocity along constant depth surfaces. It is necessary to adopt the density coordinate as the vertical axis in calculating the meridional transport streamfunction to compare modeled transports with observational estimates (McIntosh and McDougall 1996).

It is demonstrated that effects of wind forcing control intensity of the deep circulation in the Atlantic (Hasumi and Suginohara 1999b) and the middepth circulation in the Pacific (Tsujino and Suginohara 1998, 1999). However, the bottom circulation in the Atlantic and the deep circulation in the Pacific are not much affected by wind forcing (e.g., Hasumi and Suginohara 1999a). They may be “classical” thermohaline circulation, where its intensity strongly depends on vertical diffusivity (e.g., Suginohara and Aoki 1991).

What is known about vertical diffusivity? By microstructure measurements, Toole et al. (1994) and Polzin et al. (1997) obtained a diffusion coefficient of about 0.1×10^{-4} m^2 s^{-1} for the interior ocean over smooth abyssal plains and larger than 10.0×10^{-4} m^2 s^{-1} on steeply sloping boundaries or over rough bottom. Small diapycnal diffusivity at the thermocline depths is also obtained by tracer-release experiments (e.g., Ledwell et al. 1993, 1998). Vertical diffusivity is estimated also from distributions of tracers such as temperature, salinity, and ^{14}C. Munk (1966), assuming a balance between vertical advection and vertical diffusion for tracers, obtained the value of 1.3×10^{-4} m^2 s^{-1} at depths from the lower thermocline to the bottom layer. Recently, Munk and Wunsch (1998) confirmed a value larger than 10^{-4} m^2 s^{-1} as a global average. From heat budget calculation for a bottom water in a semienclosed basin introduced by Hogg et al. (1982), Roemmich et al. (1996) deduced vertical diffusivity of 500.0×10^{-4} m^2 s^{-1} near the bottom of the Samoan Passage, and Morris et al. (1997) obtained a basin-averaged vertical diffusivity of 3.0×10^{-4} m^2 s^{-1} for the bottom layer (for depths below 3500 m) of the Brazil Basin.

In the present study, we intend to reproduce the deep Pacific circulation with the observed amount of transport. Considering that vertical diffusivity increases with depth, we clarify how depth-dependent vertical diffusivity controls the

deep Pacific circulation. Vertical diffusivity is set to be 0.1×10^{-4} m^2 s^{-1} for the upper layer and 3.0×10^{-4} m^2 s^{-1} for the bottom layer in accordance with the recent estimate from various observations. We examine how the deep circulation is affected by change in diffusivity at middepths. Sensitivity of the deep circulation to vertical diffusivity in the deep layer is also examined.

There are few studies where sensitivity to depth-dependent vertical diffusivity has been investigated. Cummins et al. (1990) examined difference between a constant diffusivity case and a case with vertical diffusivity inversely proportional to the Brunt–Väisälä frequency (Gargett 1984). Cummins (1991) compared results among cases with different vertical profiles of vertical diffusivity below the thermocline. These experiments were performed for a rectangular basin in one hemisphere with a single deep-water source. Changes in density stratification and intensity of circulation were discussed: stratification is improved in the deep layer and thermohaline circulation is intensified when vertical diffusivity is allowed to increase below the thermocline. However, its mechanism is not clarified.

Since the Pacific has no deep-water source within it but has multiple deep-water sources outside of it, the situation for the Pacific may be different from a single-basin model with a single deep-water source. We carry out numerical experiments by using a World Ocean model.

This paper is organized as follows. Section 2 describes the model and the experimental design. Section 3 shows the results and clarifies effects of depth-dependent vertical diffusivity on thermohaline circulation. Section 4 presents discussion and concluding remarks.

2. Model

We use the Center for Climate System Research ocean general circulation model (CCSR-OGCM). The CCSR-OGCM is a multilevel model that solves primitive equations under the hydrostatic, Boussinesq, and rigid-lid approximation. Except for an advective tracer transport scheme, the numerical method is similar to that described by Bryan (1969). We use a high-accuracy advective tracer transport scheme, UTOPIA (Leonard et al. 1993). UTOPIA is a third-order accurate scheme that has little numerical diffusion and dispersion, which enables us to adopt such small vertical diffusivity as 0.1×10^{-4} m^2 s^{-1} for the upper layer. Performance of the CCSR-OGCM with UTOPIA is described by Hasumi and Suginohara (1999a).

Configuration of the World Ocean model is identical to that used by Hasumi and Suginohara (1999a): the horizontal resolution is about 2.8° both zonally and meridionally and there are 40 levels in the vertical.

Isopycnal diffusion (Cox 1987) is applied for the tracer equation, where the isopycnal eddy diffusion coefficient and the background horizontal eddy diffusion coefficient are chosen to be 1.0×10^3 and 1.0×10^2 m^2 s^{-1}, respectively. The coefficients for the horizontal and the vertical eddy viscosity are 3.0×10^5 and 1.0×10^{-4} m^2 s^{-1}, respectively.

Wind forcing at the sea surface is taken from the the annual-mean wind stress of Hellerman and Rosenstein (1983). Thermal and freshwater forcing at the sea surface is imposed by restoring to the winter sea surface temperature and salinity of Levitus (1982) in both hemispheres. The restoring time constant is 30 days for both temperature and salinity.

Nakata and Suginohara (1998) pointed out that the presence of the marked density stratification in the circumpolar region well below the Drake Passage sill is essential for reproducing the realistic connection between the Atlantic and the Pacific deep circulation. They imposed Newtonian body forcing in the bottom layer of the Weddell Sea. By this body forcing, AABW is realistically reproduced in a coarse-resolution model like the present one: AABW is confined to the bottom layer, forming the marked density stratification in the circumpolar region well below the Drake Passage sill. Following their suggestion, Newtonian body forcing is imposed at the southern end of the Weddell Sea below the depth of 3800 m. The body forcing is made by restoring temperature and salinity to the observed values of Levitus (1982) with the damping time of 30 days. The convective overturning scheme, which homogenizes the unstable water column, is switched off in the Weddell Sea and the Ross Sea to maintain the abyssal stratification given by the body forcing.

We carry out four cases. Vertical profiles of vertical diffusivity for cases I through IV are shown in Fig. 1. Case I is the control case where vertical diffusivity is constant at 0.3×10^{-4} m^2 s^{-1}. With vertical diffusivity at the top (25 m) and the bottom level (5400 m) fixed, 0.1×10^{-4} and 3.0×10^{-4} m^2 s^{-1}, respectively, two cases are calculated with different values in between. For case II, vertical diffusivity begins to increase with depth around 2000 m, while, for case III, it begins to increase around 500 m. Diffusivity at middepths is larger in case III than in case II. Sensitivity to vertical diffusivity in the deep layer is examined in case IV, where vertical diffusivity is the same as that in case III for the upper 1400 m but it is held constant at 1.0×10^{-4} m^2 s^{-1} for the deep layer.

The model equations are integrated for more than 6000 years to obtain a thermally and dynamically steady state, using

Bryan's (1984) acceleration method.

3. Results

a. Comparison among cases with different profiles of vertical diffusivity

The zonally integrated meridional transport streamfunction in the Pacific and the Atlantic for cases I through IV is shown in Fig. 2. All cases reproduce characteristics of meridional circulation in the World Ocean such as the deep Atlantic circulation associated with NADW formation in the northern North Atlantic, the bottom Atlantic circulation associated with AABW formation in the Weddell Sea, and the inflow of CDW into the deep Pacific.

In the Pacific, comparison among the cases reveals that the deep circulation increases in intensity for those cases where vertical diffusivity is large at middepths or in the deep layer (cases II–IV). Transport of the deep Pacific circulation for case III is the largest, about 10 Sv, which compares well with observational estimates (e.g., Schmitz 1995). The layered deep Pacific meridional circulation is formed for each case except for case I: most of the CDW that flows into the Pacific at the bottom returns to the Southern Ocean at middepths without upwelling to the sea surface. The middepth southward transport in the South Pacific exists at the depths between 2000 and 3000 m for case II, between 1000 and 3000 m for case III, and between 1000 and 2000 m for case IV. These depths are where vertical diffusivity rapidly increases with depth for each of the cases (Fig. 1). This indicates that the layered deep Pacific meridional circulation is related to the depth-dependent vertical diffusivity. When the balance between vertical advection and vertical diffusion in the temperature equation holds at middepths, which in fact is true for the Pacific as shown later, the temperature equation becomes

$$w\frac{\partial T}{\partial z} = \frac{\partial K_V}{\partial z}\frac{\partial T}{\partial z} + K_V\frac{\partial^2 T}{\partial z^2},$$

where w, T, z, and K_V represent vertical velocity, temperature, vertical coordinate (positive upward), and vertical diffusivity, respectively. At the depths where vertical diffusivity increases with depth ($\partial K_V/\partial z < 0$), the first term on the right-hand side takes a negative value, which tends to reduce the upwelling speed. The deep water that is warmed and brought up to the middepths due to intense vertical mixing cannot upwell to the upper layer, and hence it has to return horizontally to the deep-water formation region, slowly upwelling within the middepths. In other words, the small vertical diffusivity in the upper layer inhibits upwelling of the deep water across the thermocline. Thus, CDW that flows northward at the bottom returns southward to the Southern Ocean at middepths. According to Wunsch et al. (1983), the middepth southward return flow lies between 1000 and 3500 m. Here again, case III best reproduces the depths of the southward transport. Thus, for realistic reproduction of the deep Pacific circulation, vertical diffusivity needs to keep increasing with depth beginning at middepths. Just above the depths of the middepth southward transport, there is the northward transport, which forms the upper circulation cell in the layered deep Pacific meridional circulation. This thermohaline circulation cell is enhanced by wind forcing, that is, by the heating caused by Ekman upwelling in the subpolar North Pacific, as pointed out by Tsujino and Suginohara (1998, 1999).

In the Atlantic, the intensity of the deep circulation associated with NADW formation is not so different among the cases. This indicates that the intensity of the deep Atlantic circulation is controlled by a factor other than vertical diffusivity. That is, as pointed out by Hasumi and Suginohara (1999b), the deep Atlantic circulation is enhanced by the heating caused by Ekman upwelling in the Southern Ocean and its intensity is not so sensitive to vertical diffusivity. However, there are some differences: for the cases where vertical diffusivity takes a large value at depths around 1500 m (cases III and IV), the deep Atlantic circulation associated with NADW formation extends to deeper depths and increases in intensity by 3~4 Sv compared with the case where vertical diffusivity is not large there (case II). The circulation extends deeper for case III than for case IV. Thus, vertical diffusivity both at middepths and in the deep layer affects the deep Atlantic circulation as well as the deep Pacific circulation. The bottom circulation associated with AABW formation in the Weddell Sea shows little difference. The northward transport of AABW into the North Atlantic is at most 2 Sv for all cases, which is smaller than the observational estimates of about 4 Sv (e.g., McCartney and Curry 1993). Since the intensity of the bottom and the deep circulation in the Atlantic is determined by their relative strength, the strongest deep circulation in case III yields the weakest bottom circulation among the cases.

The zonally averaged density (σ_3) in the Atlantic and the Pacific for cases I through IV is shown in Fig. 3. The differences among the cases seen in meridional transport streamfunction can be explained by comparing the density fields. In the Pacific, for case II, density at depths below 2000 m is considerably homogenized. Since vertical diffusivity is large at depths only below 2000 m, the homogeneous bottom water fills the depths below 2000 m without further mixing with the upper-layer water of large heat content. Thus, for case II, the deep Pacific circulation is not intensified so much. For case III with large vertical diffusivity at middepths, however, the deep layer is significantly stratified. Since vertical diffusivity begins to increase at lower thermocline depths, heat is efficiently conducted from the upper layer to the deep layer, leading to strong stratification in the deep layer. CDW becomes warm and upwells, intensifying the meridional circulation cell below

the thermocline in the Pacific. Considering that vertical diffusivity near the bottom is the same for cases II and III, the importance of mixing between the deep water and thermocline water for reproducing the deep Pacific circulation is understood. The strong deep stratification for case IV is also caused by large vertical diffusivity at lower thermocline depths. Since vertical diffusivity is held constant below middepths, the heat from the upper layer does not penetrate so deep as that for case III, leading to the high-density, homogeneous bottom water for case IV. Thus, the strong deep circulation found for case III does not occur for case IV.

In the Atlantic, the isopycnal σ_3 = 41.4 characterizes the core of NADW. For cases III and IV, since this isopycnal is pushed down due to the intense diffusion below 1000 m, NADW reaches deeper than for case II and the deep circulation associated with NADW formation occupies depths as deep as 3500 m. For case III, the isopycnal σ_3 = 41.4 is further forced downward due to the intense diffusion in the deep layer, causing the deepest extension of the deep Atlantic circulation. This leads to the weakest bottom Atlantic circulation associated with AABW formation in the Weddell Sea: the isopycnal σ_3 = 41.5, which characterizes the northward flowing bottom water, reaches only 30°S for case III, while it reaches 30°N for cases II and IV.

We also carried out a case where vertical diffusivity is 2.0×10^{-4} m^2 s^{-1} at the bottom level for cases III and IV. The intensity of the deep Pacific circulation is that between these cases. Thus, for realistic reproduction of the deep Pacific circulation, vertical diffusivity needs to take the value as large as 3.0×10^{-4} m^2 s^{-1} in the deep layer, as well as the large value of 1.0×10^{-4} m^2 s^{-1} at middepths.

b. Role of diffusivity at middepths

It has been clearly shown in the previous subsection that vertical diffusivity that increases with depth significantly modifies both the Pacific and the Atlantic deep circulation. Especially, vertical diffusivity with a large value at middepths is important for reproducing realistic deep Pacific circulation. In this subsection, to understand how the large vertical diffusivity at middepths intensifies the deep Pacific circulation, we further compare the cases with different vertical diffusivity at mid-depths: cases II and III.

Vertical profiles of the terms in the temperature equation at depths below 800 m in the central subtropical gyre of the North Pacific and the North Atlantic for cases II and III are depicted in Fig. 4. At the shallower depths above 800 m, all of the terms, particularly the horizontal and the vertical advection term, become large because the wind-driven circulation is dominant. The balance between vertical advection and vertical diffusion in the temperature equation holds at middepths for the Pacific, while it does not for the Atlantic. This also indicates that the deep Atlantic circulation associated with NADW formation is the “wind enhanced” thermohaline circulation of Tsujino and Suginohara (1999), as demonstrated by Hasumi and Suginohara (1999b). In the Pacific, it is clearly seen that both vertical advection and vertical diffusion terms are larger for case III than case II. The larger vertical diffusivity at middepths causes the enhanced heat exchange in the deep layer as well as at middepths.

Next, differences are taken between the cases: case III minus case II (hereafter referred to the difference III − II). The zonally integrated mass transport streamfunction and zonally averaged density in σ_3 for the difference III − II in the Pacific and the Atlantic are shown in Fig. 5. In the Pacific, the meridional circulation with the northward transport of CDW at the bottom and the southward transport at middepths is intensified for case III. In the Atlantic, the deep circulation associated with NADW formation appears to be intensified by 7 Sv. About 3 Sv of the increased transport is due to an increase in the formation rate of NADW in the northern North Atlantic for case III (Fig. 2). The rest is due to the vertical extension of NADW as seen in Fig. 2. The increased portion of NADW flows out to the Southern Ocean below the depth of the Drake Passage sill. That is, the connection between the Atlantic and the Pacific deep circulation is better established for case III than for case II, as discussed by Nakata and Suginohara (1998).

In general, the density in the deep layer becomes lower (warmer) and that at the thermocline becomes higher (cooler). These features can be traced to the upper layer. At midlatitudes where the thermocline water outcrops (30°~40° in both hemispheres), the surface density is higher. In the Southern Ocean and in the northern North Atlantic where the deep water outcrops, the surface density is lower. This indicates that the buoyancy (heat) budget through the sea surface is also modified.

As seen in Fig. 5, both the deep Pacific circulation and the deep Atlantic circulation are intensified for case III. In the zonally integrated mass transport streamfunction for the difference III − II in the global ocean (Fig. 6), both the deep circulation associated with NADW formation and the bottom circulation associated with AABW formation appear to be intensified for case III. Most of the increased portion of NADW upwells only to the lower thermocline depths between 10°N and 35°S, although part of it upwells to the upper layer in the Southern Ocean. Since the increased portion of NADW flows out to the Southern Ocean without notable upwelling within the Atlantic (Fig. 5), the upwelling to the lower thermocline

depths must take place in the Pacific and Indian Oceans. Most of the increased portion of NADW flows into the Indo–Pacific sector as CDW and upwells to the lower thermocline depths, and then returns to the North Atlantic. The increased portion of AABW enhances the deep circulation in the Pacific and the Indian, as the bottom Atlantic circulation is not intensified (Fig. 5). In this way, the larger vertical diffusivity at middepths leads to enhancement of the inflow of AABW and NADW into the deep Pacific.

The effect of the larger vertical diffusivity at middepths is summarized as follows. Owing to the large vertical diffusivity at middepths, the intense mixing between the deep and lower thermocline water occurs, resulting in warming of the deep water and cooling of the thermocline water. The warmed deep water leads to the enhanced deep-water formation in the Southern Ocean and in the northern North Atlantic because of excess heat loss there. On the other hand, the cooler thermocline water leads to enhanced heat gain through the sea surface where the thermocline water outcrops to counterbalance the excess heat loss in the deep-water formation region. The enhanced vertical heat exchange at middepths causes the enhanced upwelling of the deep water to the lower thermocline depths. Since vertical diffusivity is small in the upper layer, the deep water does not further upwell to the sea surface, but flows back to the deep-water formation region, slowly upwelling within the lower thermocline depths. Thus, the intensified circulation in the deep Pacific is maintained.

c. Detailed structures for case III

We further look into the results of case III, where the deep Pacific circulation is best reproduced.

The meridional streamfunction, where zonal integration is carried out along layers of constant potential density (σ_3), for case III is shown in Fig. 7. In the Pacific, there is a 12 Sv inflow of CDW from the Southern Ocean below the isopycnal surface $\sigma_3 = 41.4$. About 2 Sv of it upwells in the South Pacific and the rest, about 10 Sv, flows into the North Pacific and upwells there. This feature resembles the circulation pattern for the deep Pacific of Schmitz (1995): 10~20 Sv of CDW enters the South Pacific and 10 Sv of it crosses the equator. About 8 Sv of the upwelled water returns to the Southern Ocean at depths between 1500 and 3000 m (Fig. 2). This deep Pacific circulation compares well with the result of Wunsch et al. (1983) in both depth and intensity. The meridional streamfunction in Fig. 2 yields a 10 Sv inflow of CDW into the South Pacific, while that in Fig. 7 yields 12 Sv. The contour line of 10 Sv is isolated in Fig. 2, while it is continuous in Fig. 7. We need to adopt the density coordinate as the vertical axis when model results are compared with observational estimates. This is important especially when large vertical diffusivity is taken for the deep layer. The strong vertical mixing causes intense water mass modification, leading to the large zonal gradient of isopycnals with respect to the surface of constant depth.

Only a small amount of the deep water upwells across $\sigma_3 = 41.2$ in the South Atlantic, while uniform upwelling across this isopycnal occurs in the entire Pacific. The upwelling across this isopycnal seen in the North Atlantic is largely due to diapycnal diffusion at the western boundary caused by the horizontal diffusion (e.g., Böning et al. 1995). Since the deep Atlantic circulation associated with formation of NADW is a wind-enhanced thermohaline circulation (Hasumi and Suginohara 1999b), most of the NADW flows into the Southern Ocean without notable upwelling on the way. Part of the NADW flows into the Indo–Pacific sector and upwells to lower thermocline depths as the classical thermohaline circulation. Thus, characteristics of the deep thermohaline circulation in each basin strongly depend upon whether they are dominated by a wind-enhanced thermohaline circulation or not.

Horizontal velocity fields at depths of 2400 and 4200 m for case III are shown in Fig. 8. At 2400 m in the Pacific there exists the southward flow continuing from the North Pacific to the Southern Ocean. It forms the western boundary current in the South Pacific and separates from the western boundary at about 40°S. This southward flow represents the middepth southward transport that brings silicate-rich deep water from the North Pacific to the South Pacific (Wunsch et al. 1983). As seen at 4200 m, the bottom water is formed only in the Weddell Sea because the body forcing is imposed there, and it flows into all basins, forming the northward western boundary currents.

Zonal sections of meridional velocity along 11.1°, 27.7°, and 44.3°S are shown in Fig. 9. In the deep Pacific around 160°W there exists the strong northward western boundary current. This current corresponds to the inflow of CDW, which resembles Warren's (1973) observation in both depth and structure. Just above and to the east of the northward flow exists the southward flow. The core of the southward flow lies around a depth of 2500 m, close to Wunsch et al.'s (1983) estimate.

Meridional sections of salinity in the central Pacific (170.2°W) and Atlantic (26.7°W), along with the annual mean climatology of Levitus (1982), are plotted in Fig. 10. In the Pacific, though salinity in the deep layer is slightly lower than the observed, the basic feature of salinity distribution is well reproduced: there are salinity minima at the intermediate depths in the Northern and Southern Hemispheres and the deep salinity maximum in the Southern Hemisphere. The deep salinity maximum in the Southern Hemisphere indicates that high salinity water originating from the NADW flows into the Pacific; that is, the connection between the Atlantic and the Pacific deep water through the Southern Ocean is realistically

established. Part of the NADW that flows into the Southern Ocean from the Atlantic below the Drake Passage sill depth is well mixed with AABW by strong vertical diffusion in the Southern Ocean to form CDW with a high salinity signal on its top. In the Atlantic, the intrusion of high salinity NADW into the Southern Ocean is weak, which leads to the low salinity in the deep Pacific. This is partly due to the low salinity in the upper layer of the Weddell Sea, which is caused by deep convective penetration of low-salinity surface water north of the Weddell Sea. The exact representation of the bottom-water formation process in the Weddell Sea will improve the salinity distribution.

4. Discussion and concluding remarks

In the present study, the deep Pacific circulation has been investigated by using a World Ocean model. Depth-dependent vertical diffusivity is employed to control the circulation. Vertical diffusivity estimated from observations is adopted, that is, 0.1×10^{-4} m^2 s^{-1} for the upper layer and 3.0×10^{-4} m^2 s^{-1} for the bottom layer. Comparison is made between two cases with different vertical diffusivity at middepths, where vertical diffusivity is uncertain. With larger vertical diffusivity at middepths, the deep Pacific circulation is intensified and its pattern becomes realistic, forming the layered deep Pacific meridional circulation. This circulation yields tracer distributions that compare well with observations. Such a strong deep Pacific circulation does not occur when vertical diffusivity is taken larger at middepths but is held constant below the middepths. Thus, it is found that for realistic reproduction of the deep Pacific circulation, vertical diffusivity needs to be depth dependent and to take the large value of 1.0×10^{-4} m^2 s^{-1} at the lower thermocline depths and the value as large as 3.0×10^{-4} m^2 s^{-1} in the bottom layer.

When vertical diffusivity is taken to increase with depths beginning at the lower thermocline depths, NADW and AABW are well mixed to form CDW due to the strong vertical diffusion in the deep layer of the Southern Ocean. The CDW that flows into the Pacific upwells to lower thermocline depths due to the enhanced heat exchange with the thermocline water through the large vertical diffusivity there. The water below the thermocline is warmed and the thermocline water is cooled for the whole basin. The warmed deep water leads to enhanced deep-water formation in the deep-water formation region due to excess heat loss through the sea surface, while the cooled thermocline water leads to excess heat gain through the sea surface where the thermocline water outcrops, counterbalancing the excess heat loss in the deep-water formation region. The deep water brought up to lower thermocline depths does not further upwell to the sea surface due to the small upper-layer vertical diffusivity, but it flows back to the Southern Ocean, slowly upwelling within the lower thermocline depths. In this way, the meridional overturning with larger transport forms in the deep Pacific. This mechanism carries over to the results of Cummins's (1991) experiments where a rectangular basin in one hemisphere with a single deep-water source is considered. Thus, the deep Pacific circulation is considered to be the classical thermohaline circulation where its strength is dependent strongly on vertical diffusivity. This makes a remarkable contrast to the deep Atlantic circulation associated with NADW formation, which is the wind-enhanced thermohaline circulation of Tsujino and Suginohara (1999) as demonstrated by Hasumi and Suginohara (1999b).

Although the deeper extension of the deep Atlantic circulation due to the large vertical diffusivity at middepths improves the connection between the Atlantic and the Pacific deep circulation, representation of a realistic formation process of AABW is important for reproducing the realistic connection as demonstrated by Nakata and Suginohara (1998). In the present model, the formation process of AABW in the Weddell Sea is externally prescribed by the body forcing at the bottom level. The body forcing yields the realistic bottom circulation with the marked density stratification well below the Drake Passage sill. Cases without body forcing show that the deep Atlantic is less stratified, leading to a much smaller amount of NADW entering the deep Pacific compared with cases with body forcing,

Though horizontally uniform vertical diffusivity is adopted in the present study, observations indicate that vertical diffusivity varies both vertically and horizontally (e.g., Toole et al. 1994; Polzin et al. 1997). Numerical experiments with enhanced vertical diffusivity near the coastal boundaries (Marotzke 1997; Samelson 1998) and over rough bathymetry (Hasumi and Suginohara 1999c) demonstrated that stratification and circulation for the locally enhanced diffusivity case are significantly different from those for the uniform mixing case, while the intensity of thermohaline circulation is not so different when the zonal integral of vertical diffusivity is the same. Thus, knowledge of the three-dimensional distribution of vertical diffusivity is indispensable to reproduce a realistic circulation in OGCMs.

Acknowledgments

We would like to thank Ryo Furue, Hideyuki Nakano, and Akira Oka for pleasant discussions. Comments given by J. R. Toggweiler as well as an additional anonymous reviewer helped improve our manuscript. All the figures are drawn with graphic routines in the GFD-Dennou Library, developed by the GFD-Dennou Club.

REFERENCES

Böning, C. W., W. R. Holland, F. O. Bryan, G. Danabasoglu, and J. C. McWilliams, 1995: An overlooked problem in model simulations of the thermohaline circulation and heat transport in the Atlantic Ocean. *J. Climate,* **8,** 515–523. Find this article online

Bryan, K., 1969: A numerical method for the study of the circulation of the world ocean. *J. Comput. Phys.,* **4,** 347–376.

— ,1984: Accelerating the convergence to equilibrium of ocean–climate models. *J. Phys. Oceanogr.,* **14,** 666–673. Find this article online

— ,and L. J. Lewis, 1979: A water mass model of the world ocean. *J. Geophys. Res.,* **84,** 2503–2517.

Cox, M. D., 1987: Isopycnal diffusion in a *z*-coordinate ocean model. *Ocean Modelling* (unpublished manuscripts), **74,** 1–5.

Cummins, P. F., 1991: The deep water stratification of ocean general circulation models. *Atmos.–Ocean,* **29,** 563–575.

— ,G. Holloway, and A. E. Gargett, 1990: Sensitivity of the GFDL ocean general circulation model to a parameterization of vertical diffusion. *J. Phys. Oceanogr.,* **20,** 817–830. Find this article online

England, M. H., 1993: Representing the global-scale water masses in ocean general circulation models. *J. Phys. Oceanogr.,* **23,** 1523–1552. Find this article online

Gargett, A. E., 1984: Vertical eddy diffusivity in the ocean interior. *J. Mar. Res.,* **42,** 359–393.

Hasumi, H., and N. Suginohara, 1999a: Sensitivity of a global ocean general circulation model to tracer advection schemes. *J. Phys. Oceanogr.,* **29,** 2730–2740. Find this article online

— ,and — ,1999b: Atlantic deep circulation controlled by heating in the Southern Ocean. *Geophys. Res. Lett.,* **26,** 1873–1876.

— ,and — ,1999c: Effects of locally enhanced vertical diffusivity over rough bathymetry on the world ocean circulation. *J. Geophys. Res.,* **104,** 23 367–23 374.

Hellerman, S., and M. Rosenstein, 1983: Normal monthly wind stress over the world ocean with error estimates. *J. Phys. Oceanogr.,* **13,** 1093–1104. Find this article online

Hogg, N. G., P. Biscaye, W. Gardner, and W. J. Schmitz, 1982: On the transport and modification of Antarctic Bottom Water in the Vema Channel. *J. Mar. Res.,* **40** (Suppl.), 231–263.

Ledwell, J. R., A. J. Watson, and C. S. Law, 1993: Evidence for slow mixing across the pycnocline from an open-ocean tracer-release experiment. *Nature,* **364,** 701–703.

— ,— ,and — ,1998: Mixing of a tracer in the pycnocline. *J. Geophys. Res.,* **103,** 21 499–21 529.

Leonard, B. P., M. K. MacVean, and A. P. Lock, 1993: Positivity-preserving numerical schemes for multidimensional advection. NASA Tech. Memo. 106055, ICOMP-93-05, 62 pp.

Levitus, S., 1982: *Climatological Atlas of the World Ocean.* NOAA Prof. Paper No. 13, U.S. Govt. Printing Office, Washington, DC, 173 pp.

Maier-Reimer, E., U. Mikolajewicz, and K. Hasselmann, 1993: Mean circulation of the Hamburg LSG OGCM and its sensitivity to the thermohaline surface forcing. *J. Phys. Oceanogr.,* **23,** 731–757. Find this article online

Marotzke, J., 1997: Boundary mixing and dynamics of three-dimensional thermohaline circulation. *J. Phys. Oceanogr.,* **27,** 1713–1728. Find this article online

McCartney, M. S., and R. A. Curry, 1993: Transequatorial flow of Antarctic Bottom Water in the western Atlantic Ocean: Abyssal geostrophy at the equator. *J. Phys. Oceanogr.,* **23,** 1264–1276. Find this article online

McIntosh, P. C., and T. J. McDougall, 1996: Isopycnal averaging and the residual mean circulation. *J. Phys. Oceanogr.,* **26,** 1655–1660. Find this article online

Morris, M., N. G. Hogg, and W. B. Owens, 1997: Diapycnal mixing estimated from advective budgets in the deep Brazil Basin. *WOCE Newsletter,* No. 28, 23–25.

Munk, W. H., 1966: Abyssal recipes. *Deep-Sea Res.,* **13,** 707–730.

— ,and C. Wunsch, 1998: Abyssal recipes II: Energetics of tidal and wind mixing. *Deep-Sea Res. I,* **45,** 1977–2010.

Nakata, M., and N. Suginohara, 1998: Role of deep stratification in transporting deep water from the Atlantic to the Pacific. *J. Geophys.*

Res., **103,** 1067–1086.

Obata, A., R. Furue, S. Aoki, and N. Suginohara, 1996: Modeling layered structure in deep Pacific circulation. *J. Geophys. Res.*, **101,** 3663–3674.

Polzin, K. L., J. M. Toole, J. R. Ledwell, and R. W. Schmitt, 1997: Spatial variability of turbulent mixing in the abyssal ocean. *Science*, **276,** 93–96.

Roemmich, D., T. McCallister, and J. Swift, 1991: A transpacific hydrographic section along latitude 24°N: The distribution of properties in the subtropical gyre. *Deep-Sea Res.*, **38** (Suppl. 1), S1–S20.

— ,S. L. Hautala, and D. L. Rudnick, 1996: Northward abyssal transport through the Samoan Passage and adjacent regions. *J. Geophys. Res.*, **101,** 14 039–14 055.

Rudnick, D. L., 1997: Direct velocity measurements in the Samoan Passage. *J. Geophys. Res.*, **102,** 3293–3302.

Samelson, R. M., 1998: Large-scale circulation with locally enhanced vertical mixing. *J. Phys. Oceanogr.*, **28,** 712–726. Find this article online

Schmitz, W. J., 1995: On the interbasin-scale thermohaline circulation. *Rev. Geophys.*, **33,** 151–173.

Suginohara, N., and S. Aoki, 1991: Buoyancy-driven circulation as horizontal convection on β-plane. *J. Mar. Res.*, **49,** 295–320.

Toggweiler, J. R., and B. Samuels, 1993: New radiocarbon constraints on the upwelling of abyssal water to the ocean's surface. *The Global Carbon Cycle*, M. Heimann, Ed., NATO-ASI Series, Springer-Verlag, 333–366.

Toole, J. M., K. L. Polzin, and R. W. Schmitt, 1994: Estimates of diapycnal mixing in the abyssal ocean. *Science*, **264,** 1120–1123.

Tsujino, H., and N. Suginohara, 1998: Thermohaline effects on upper layer circulation of the North Pacific. *J. Geophys. Res.*, **103,** 18 665–18 679.

— ,and — ,1999: Thermohaline circulation enhanced by wind forcing. *J. Phys. Oceanogr.*, **29,** 1506–1516. Find this article online

Warren, B. A., 1973: Transpacific hydrographic sections at Lats. 43°S and 28°S: The SCORPIO Expedition—II. Deep water: *Deep-Sea Res.*, **20,** 9–38.

Wijffels, S. E., J. M. Toole, H. L. Bryden, R. A. Fine, W. J. Jenkins, and J. L. Bullister, 1996: The water masses and circulation at 10°N in the Pacific. *Deep-Sea Res. I*, **43,** 501–544.

Wunsch, C., D. Hu, and B. Grant, 1983: Mass, heat, salt and nutrient fluxes in the South Pacific Ocean. *J. Phys. Oceanogr.*, **13,** 725–753. Find this article online

---

Figures

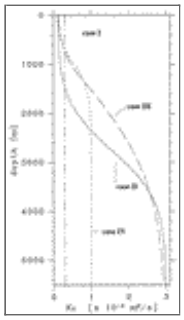

Click on thumbnail for full-sized image.

Fig. 1. Vertical profiles of vertical diffusivity for cases I through IV

Click on thumbnail for full-sized image.

Fig. 2. Zonally integrated mass transport streamfunction for (a) the Pacific and (b) the Atlantic in Sverdrups (Sv $\equiv 10^6$ m^3 s^{-1}). Contour interval is 2 Sv

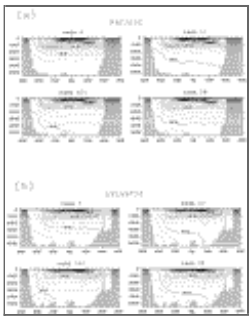

Click on thumbnail for full-sized image.

Fig. 3. Zonally averaged potential density (in σ_3) for (a) the Pacific and (b) the Atlantic. Contour interval is $0.25\sigma_3$. For density greater than $41.0\sigma_3$, contour interval is $0.1\sigma_3$

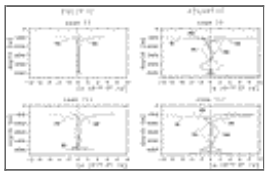

Click on thumbnail for full-sized image.

Fig. 4. Vertical profiles of the terms in the temperature equation at the depths below 800 m in the central subtropical gyre of the North Pacific (29.0°N, 170.2°E) and the North Atlantic (29.0°N, 54.8°W) for cases II and III: HA; horizontal advection, VA: vertical advection; VD: vertical diffusion; HD; horizontal diffusion, and ID; isopycnal diffusion. The unit of the abscissa is deg s^{-1}

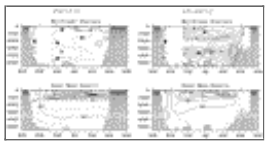

Click on thumbnail for full-sized image.

Fig. 5. Zonally integrated mass transport streamfunction (in Sv) and zonally averaged potential density (in σ_3) for the difference III − II. Contour interval is 1 Sv for streamfunction and $0.05\sigma_3$ for density

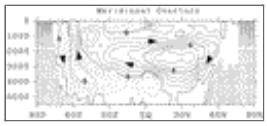

Click on thumbnail for full-sized image.

Fig. 6. Zonally integrated mass transport streamfunction of the global ocean (in Sv) for the difference III − II. Contour interval is 1 Sv

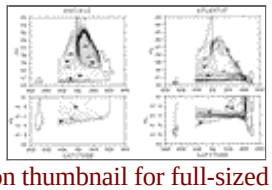

Click on thumbnail for full-sized image.

Fig. 7. Meridional streamfunction (in Sv) for case III. Zonal integration has been carried out along layers of constant potential density (in σ_3). Contour interval is 2 Sv

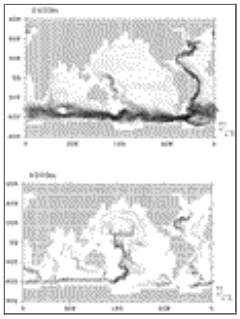

Click on thumbnail for full-sized image.

Fig. 8. Horizontal velocity fields at 2400 and 4200 m for case III. Unit vector is 4.0 cm s^{-1} for 2400 m and 2.0 cm s^{-1} for 4200 m. Blank areas indicate that the bottom is shallower than the depth

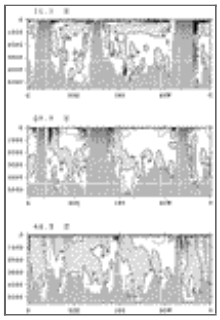

Click on thumbnail for full-sized image.

Fig. 9. Zonal sections of meridional velocity for case III along 11.1°, 27.7°, and 44.3°S. Contour interval is 0.5 cm s^{-1}. The shaded regions indicate the southward flow

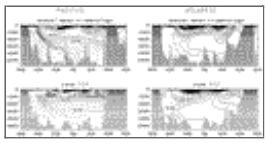

Click on thumbnail for full-sized image.

Fig. 10. Meridional sections of salinity along 170°W in the Pacific and along 27°W in the Atlantic for the Levitus (1982) climatology (above) and case III (below) in psu. Contour interval is 0.1 psu. For the 170°W, section, contour interval between 34.6 psu and 34.75 psu is 0.01 psu for climatology and contour interval between 34.4 psu and 34.6 psu is 0.01 psu for case III

Corresponding author address: Dr. Hiroyuki Tsujino, Center for Climate System Research, University of Tokyo, 4-6-1 Komaba, Meguro-ku, 153-8904 Tokyo, Japan. E-mail: tsujino@ccsr.u-tokyo.ac.jp

top